

Crystal Structure and Polarized Electronic Spectra of a (μ -Superoxo)dicobalt(III) Complex: $[(\text{NH}_3)_5\text{Co}]_2\text{O}_2(\text{NO}_3)_2\text{Cl}_3 \cdot 2\text{H}_2\text{O}$

VINCENT M. MISKOWSKI,* BERNARD D. SANTARSIERO, WILLIAM P. SCHAEFER, GARY E. ANSOK,
and HARRY B. GRAY*

Received April 7, 1983

The crystal structure of $[(\text{NH}_3)_5\text{Co}]_2\text{O}_2(\text{NO}_3)_2\text{Cl}_3 \cdot 2\text{H}_2\text{O}$ has been determined. The compound crystallizes in the orthorhombic space group $Pnmm$ (No. 58) with $a = 17.367$ (4) Å, $b = 8.735$ (3) Å, $c = 6.951$ (2) Å, and $Z = 2$. The cation has crystallographic C_{2h} symmetry. Single-crystal electronic spectra for 300 nm $< \lambda < 900$ nm were obtained for light polarized parallel to each of the orthorhombic axes. A weak unstructured band at 800 nm is polarized parallel to the O-O axis and assigned to the superoxide-localized $\pi_h^* \rightarrow \pi_v^*$ transition. An intense (ϵ isotropic) ~ 800 band at 680 nm is polarized parallel to Co-Co and structured in 700- and 400-cm $^{-1}$ vibrations, which are assigned to excited-state $\nu(\text{O}_2)$ and $\nu(\text{Co-O})$ modes. The excited state is peroxide-like; thus, the transition is assigned as metal-to-ligand charge transfer (MLCT), $d_{xz} \rightarrow \pi_v^*$. A much weaker but similarly structured transition at 550 nm is also assigned as $d_{xz} \rightarrow \pi_v^*$. Bands with ϵ 100-300 are observed at 480 and 464 nm, with polarizations \parallel Co-O and \perp Co-O, respectively. The latter shows a long progression in a 420-cm $^{-1}$ excited-state vibration, assigned as the equatorial Co-N stretch. The bands are assigned as the ${}^1A_1 \rightarrow {}^1E$ and ${}^1A_1 \rightarrow {}^1A_2$ components of the cobalt-localized ${}^1A_1 \rightarrow {}^1T_1$ ligand field transition. A shoulder at 350 nm in the parallel-to-molecular- C_2 spectrum is assigned to the ${}^1A_1 \rightarrow {}^1B_2$ component of the ${}^1A_1 \rightarrow {}^1T_2$ ligand field transition.

Introduction

In 1975 we published detailed assignments of the electronic spectra of (μ -superoxo)dicobalt(III) complexes.¹ Our aim at the time was to elucidate the electronic energy levels of relatively simple complexes of the O₂ unit to a degree that would assist in the analysis of the electronic structures and spectra of biologically important metal-O₂ systems. The experimental information at the time was limited to isotropic low-temperature spectra, mainly in aqueous glasses, and the assignments were based on our interpretation of perturbations induced by ligand and oxidation-state variations.

We recognized from the beginning that more conclusive information might be gained from low-temperature single-crystal polarized spectra but were unable to obtain suitable samples. We have now prepared and structurally characterized a $[(\text{Co}(\text{NH}_3)_5)_2\text{O}_2]^{5+}$ salt that is ideally suited for single-crystal polarized spectral analysis. Because the extremely complex electronic spectra of the μ -superoxo complexes remain one of the more informative probes of the bonding interactions of O₂ with metal ions, we have performed a study of the polarized spectra of this salt and report our results herein.

Experimental Section

The compound $[(\text{Co}(\text{NH}_3)_5)_2\text{O}_2(\text{NO}_3)_2\text{Cl}_3 \cdot 2\text{H}_2\text{O}]$ was obtained fortuitously in the course of attempts to grow large crystals of the pentanitrato salt. To a warm (50 °C) concentrated solution of $[(\text{Co}(\text{NH}_3)_5)_2\text{O}_2]\text{Cl}_5^{2-}$ in 1 M aqueous acetic acid (~ 500 mL) was added dropwise, with rapid stirring, 5 mL of concentrated nitric acid. The solution was set aside for several days, resulting in the growth of shiny black crystals up to several centimeters in their largest dimension. Thin bladelike crystals predominated; the major face was identified as (100) by X-ray photographic methods. The thin crystals were light yellow and turquoise, respectively, when viewed with light polarized parallel to c (the long crystal axis) and parallel to b .

Preliminary X-ray photographs indicated an orthorhombic cell, and the systematic absences of $0kl$, $k + l = 2n + 1$, and $h0l$, $h + l = 2n + 1$, indicated possible space groups $Pnmm$ (No. 58) and $Pnn2$ (No. 34). The centric space group was chosen on the basis of intensity statistics and confirmed by the successful structure solution. Cell dimensions were obtained by a least-squares fit to the setting angles of 15 reflections with $11^\circ < 2\theta < 27^\circ$. The measured density (1.84 (1) g cm $^{-3}$) compares well with the X-ray density (1.847 (1) g cm $^{-3}$).

Data were collected on a locally modified Syntex P2₁ diffractometer using graphite-monochromated Mo K α radiation ($\lambda = 0.71069$ Å)

Table I. Final Atomic Parameters^a

atom	x	y	z	B, ^b Å ²
Co	1069.0 (1)	1523.2 (3)	0	1.28 (3)
O	363 (1)	9842 (2)	0	2.36 (3)
N1	1871 (1)	3074 (2)	0	2.05 (3)
N2	521 (1)	2647 (2)	1987 (2)	2.16 (2)
N3	1608 (1)	382 (2)	2008 (2)	2.13 (2)
N4	3726 (1)	1620 (3)	0	2.72 (3)
O1N4	4321 (1)	869 (3)	0	3.93 (4)
O2N4	3406 (1)	2015 (2)	1540 (2)	3.87 (3)
OW	954 (1)	5948 (3)	0	3.14 (3)
Cl1	1/2	1/2	0	2.47 (1)
Cl2	7088 (1)	1900 (1)	0	2.60 (1)
H1N1	1666 (20)	3983 (43)	0	5.2 (9)
H2N1	2182 (15)	3013 (33)	956 (42)	7.6 (9)
H1N2	182 (15)	3266 (29)	1571 (40)	6.1 (7)
H2N2	837 (14)	3198 (28)	2781 (41)	5.1 (6)
H3N2	294 (16)	2087 (37)	2782 (44)	6.4 (8)
H1N3	1809 (14)	981 (29)	2866 (37)	5.3 (6)
H2N3	1985 (14)	9771 (30)	1624 (37)	5.1 (6)
H3N3	1251 (14)	9831 (32)	2623 (39)	5.9 (7)
HW	1163 (14)	6322 (31)	905 (40)	6.5 (8)

^a Positional parameters have been multiplied by 10⁴. ^b $B_{\text{eq}} = 8\pi^2 U_{\text{eq}}$. $U_{\text{eq}} = (U_{11}U_{22}U_{33})^{1/3}$; $\sigma(U_{\text{eq}}) = (1/6^{1/2})(\sigma U_{ij}/U_{ij})U_{\text{eq}}$.

Table II. Selected Distances (Å) and Angles (deg)

Co-O	1.913 (2)	Co-O-O	117.6 (1)
Co-N1	1.943 (2)	O-Co-N1	174.1 (1)
Co-N2	1.944 (2)	O-Co-N2	94.2 (1)
Co-N3	1.955 (2)	O-Co-N3	85.2 (1)
O-O	1.290 (2)		

and a crystal $0.3 \times 0.4 \times 0.4$ mm. Reflections with $3^\circ < 2\theta < 55^\circ$ were scanned (θ - 2θ mode) at $2^\circ/\text{min}$ with background counted at each end of the scan for half the scan time. The 2393 reflections measured (including 3 check reflections measured every 97 reflections) were merged to give 2066 independent reflections, of which 1996 has $F_o^2 > 0$ and 1674 had $F_o^2 > 3\sigma(F_o^2)$. The data were corrected for Lorentz and polarization factors but not for absorption ($\mu = 20.8$ cm $^{-1}$, $\mu_{\text{r,max}} = 0.67$).

The structure was solved by Patterson and Fourier methods and refined by least squares with use of programs of the CRYM system to a final R index of 0.037 ($R = \sum |F_o - |F_c|| / \sum F_o$) for all positive reflections and 0.028 for those with $F_o^2 > 3\sigma(F_o^2)$. The goodness of fit is 1.54 ($\text{GOF} = [\sum w(F_o^2 - F_c^2)^2 / (n - p)]^{1/2}$; $n = 2066 =$ number of data, $p = 110 =$ number of parameters). Final values for the atomic parameters are given in Table I; important bond lengths and angles are in Table II. The structure of the cation closely resembles that found in earlier determinations.³

(1) Miskowski, V. M.; Robbins, J. L.; Treitel, I. M.; Gray, H. B. *Inorg. Chem.* 1975, 14, 2318.

(2) Linhard, M.; Weigel, M. Z. *Anorg. Allg. Chem.* 1961, 308, 254.

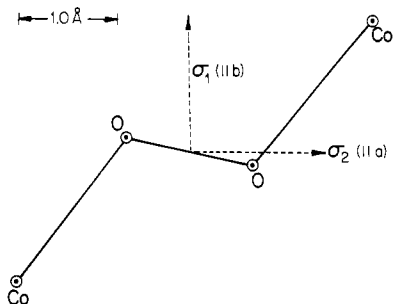


Figure 1. Schematic diagram of the Co_2O_2 unit in the (001) plane, showing the orientation of the experimental polarization data.

Table III. Calculated Relative Intensities for Electric Dipole Transition Moments

moment	σ_2	σ_1	π
$\parallel \text{O}-\text{O}$	0.96	0.04	0
$\parallel \text{Co}-\text{Co}$	0.66	0.34	0
$\parallel \text{Co}-\text{O}$	0.41	0.59	0
$\perp \text{Co}-\text{O}$	0.59	0.41	1.0

Polarized spectra were obtained for a series of crystals of thickness ranging from 190 μm to less than 10 μm . Thicknesses were measured with a calibrated microscope scale; this was not very precise for the thinnest crystals. Since Beer's law was accurately obeyed by the thicker crystals, we have assumed that the correlation extends to the thinnest crystals, so as to obtain reasonably precise estimates of extinction coefficients for the most intense bands. Thin crystals were obtained by polishing large crystals with alumina powder. Care was taken to select crystal regions that showed uniform interference colors between crossed polarizers. All crystals were carefully masked off with heat-conducting copper grease. Because of the large surface areas of even the very thin crystals, we had no difficulty maintaining our Cary 17 slit widths much less than the horizontal crystal dimensions for λ in the range 300–880 nm. Nitrate anion absorption is negligibly small in this region.

We also required polarized spectra for the (010) face. Since this face was not developed on the crystals, it was obtained by polishing very large crystals. When polished thin, the crystals nearly always showed cracks parallel to c ; by sheer persistence, a few thin samples suitable for room-temperature spectra were obtained. They were light yellow and dark cobalt blue when viewed with light polarized respectively parallel to c and parallel to a . Unfortunately, all of these samples developed cracks (hence, light leaks) when cooled for low-temperature measurements.

Low-temperature spectra showed negligible change below about 25 K. All low-temperature structure claimed in this paper has been observed for at least three different crystals with thicknesses varying by at least a factor of 2.

Crystal Considerations

The C_{2h} site symmetry of the $[(\text{Co}(\text{NH}_3)_5)_2\text{O}_2]^{5+}$ ion in the orthorhombic crystals of the title compound conforms to the maximal free-ion symmetry. The crystal c axis is parallel to the ion C_2 axis, and electric dipole allowed transitions divide neatly into those transforming (C_{2h} labels) as A_u , allowed for light polarized parallel to c , and B_u , allowed for polarization perpendicular to c . By convention, we will refer to the $\parallel c$ and $\perp c$ polarizations as π and σ , respectively. A B_u transition can in principle be polarized in any direction perpendicular to c . We have obtained polarized spectra for two orthogonal directions perpendicular to c , $\parallel b$ and $\parallel a$. We designate these as σ_1 and σ_2 , respectively. Figure 1 shows the relationship of σ_1 and σ_2 to the cation orientation. For any given σ -polarized transition, the angle its transition moment makes with the a axis is defined by $\tan^2 \theta = \epsilon(\sigma_1)/\epsilon(\sigma_2)$. In Table III we list relative intensities in the different polarizations calculated for

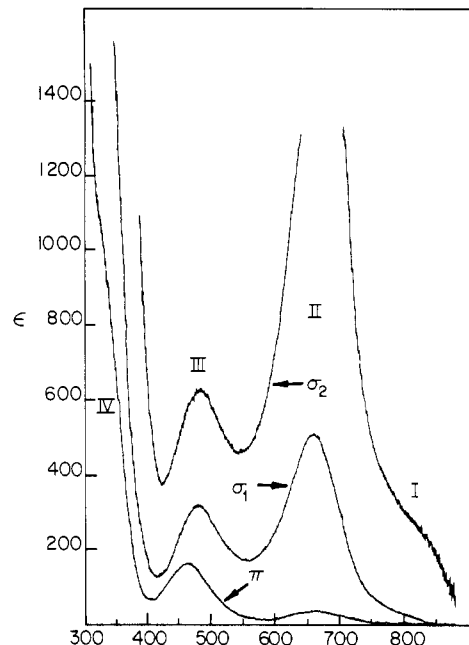


Figure 2. Room-temperature electronic absorption spectra for $[(\text{NH}_3)_5\text{Co}_2\text{O}_2](\text{NO}_3)_2\text{Cl}_3 \cdot 2\text{H}_2\text{O}$ crystals. The crystal from which the π and σ_1 data were obtained was 6.1 μm thick. The crystal from which the σ_2 data were obtained was 8.2 μm thick.

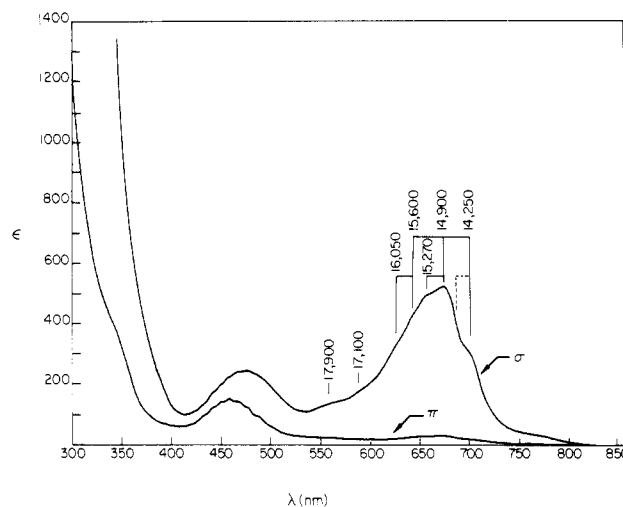


Figure 3. Spectra of crystals (described in Figure 2) at 15 K. Energies of vibronic features are indicated in cm^{-1} .

several different assumed transition moment orientations. The third entry corresponds to a transition polarized along the local approximate C_4 axis of the $\text{Co}^{\text{III}}(\text{NH}_3)_5\text{O}$ unit, and the last entry in Table III indicates relative intensities calculated for an "e" transition polarized perpendicular to this local C_4 axis. Since all of the σ -polarized transitions can mix with each other, real examples cannot be expected to agree exactly with any of the entries in Table III.

Electronic Spectra

Room- and low-temperature polarized spectra are displayed in Figures 2 and 3, and an expanded portion of the π spectrum is shown in Figure 4. Identical π spectra were obtained for the (100) and (010) crystal faces. Our room-temperature data are reasonably consistent with the pioneering study of the nitrate salt by Yamada et al.⁴ for $\lambda \gtrsim 400$ nm. There are problems with Yamada's results at shorter wavelengths, owing

(3) Schaefer, W. P.; Marsh, R. E. *Acta Crystallogr.* **1966**, *21*, 735. Marsh, R. E.; Schaefer, W. P. *Acta Crystallogr., Sect. B* **1968**, *B24*, 246. Schaefer, W. P.; Ealick, S. E.; Marsh, R. E. *Ibid.* **1981**, *B37*, 34.

(4) Yamada, S.; Shimura, Y.; Tsuchida, R. *Bull. Chem. Soc. Jpn.* **1953**, *26*, 533.

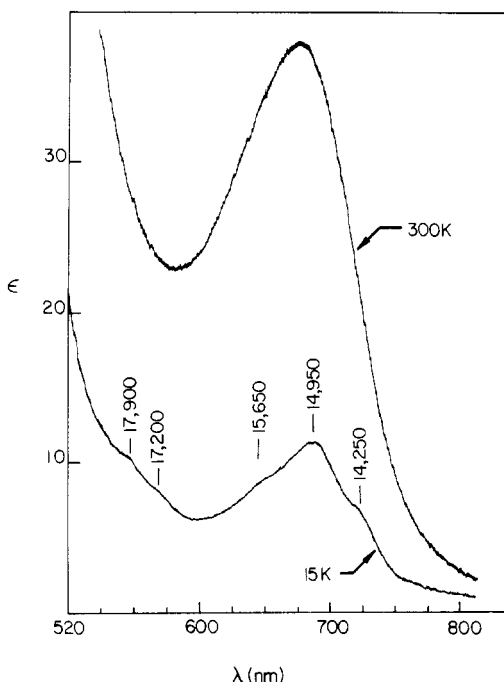


Figure 4. Absorption spectra in π polarization for a 97 μm thick $[(\text{NH}_3)_5\text{Co}]_2(\text{O}_2)(\text{NO}_3)_2\text{Cl}_3 \cdot 2\text{H}_2\text{O}$ crystal. Energies of vibronic features are indicated in cm^{-1} .

to instrumental deficiencies.⁵

We initially note that the cation in the crystal has a visible spectrum very similar to that of solutions. Earlier we reported¹ room-temperature values of $\lambda_{\text{max}}(\epsilon)$ as follows: 800 nm (~ 110 , sh), 671.5 nm (927), 480 nm (309). The crystal isotropic spectrum is simply the average of π , σ_1 , and σ_2 . We were not able to obtain a crystal thin enough to measure the entire σ_2 spectrum. Assuming that the band near 650 nm (Figure 2) has the same shape in σ_2 as in σ_1 , we estimate $\epsilon_{\text{max}}(\sigma_2) \approx 1800$ and calculate the crystal isotropic $\lambda_{\text{max}}(\epsilon)$ values to be the following: 800 nm (~ 105 , sh), 662 nm (~ 800), 480 nm (370). Thus, we are confident that we are dealing with the chromophore that was studied previously in solution.

In Figure 2 we have labeled four "systems" of absorption I-IV. All of these were assigned in our earlier paper.¹ The molecular orbitals involved in the assigned transitions are (see Figure 5 of ref 1) the filled $d\pi$ orbitals of Co(III) (xz , yz , and $x^2 - y^2$),⁶ the π^* orbitals of O_2^- (split into the filled in-plane π_h^* and the half-filled out-of-plane π_v^*), and the empty $d\sigma^*$ Co(III) orbitals (z^2 and xy). In the following we discuss our new data for each of these systems in turn.

System I

System I, a relatively weak shoulder both in the crystal and in solution, failed to show any vibronic structure at low temperature. In ref 1, following detailed reasoning which will not be repeated here, system I was assigned to the " O_2 -localized" transition $\pi_h^* \rightarrow \pi_v^*$, ${}^2B_g \rightarrow {}^2A_g$. The sole piece of new information provided by the present work is that system I appears nearly exclusively in σ_2 polarization, consistent with polarization along O-O (Table III), and thus with O_2 localization. This transition is expected to be purely vibronically allowed in C_{2h} site symmetry and should therefore display decreased integrated intensity at low temperatures. Unfortunately, pronounced narrowing of the much more intense system II obscures the temperature behavior of system I.

The absence of resolved vibronic structure in system I conceivably reflects a tendency for the excited state to adopt a nonplanar structure. The analogous transition of HO_2^- (electronic origin at 7000 cm^{-1})⁷ is nicely structured.

System II

In ref 1 we assigned system II to an MLCT (metal-to-ligand charge transfer) transition, $\text{Co}(d\pi) \rightarrow \pi_v^*$. Our new data are totally in accord with this assignment.

System II is strongly σ polarized (Figures 2 and 3). Moreover, the weak π intensity is predominantly vibronically induced, as it shows a very large decrease with decreasing temperature (Figure 4). If the σ_2 room-temperature ϵ of system II is estimated to be 1800, as indicated previously, the $\epsilon(\sigma_1)/\epsilon(\sigma_2)$ ratio is ~ 0.3 . This is most consistent with polarization parallel to the Co-Co vector (Table III) but indicates rotation toward the O-O vector by $\sim 7^\circ$, which is reasonable for a charge-transfer transition, as π_v^* is highly delocalized.

System II shows diffuse vibronic structure. The predominant feature is a short progression in $\Delta\tilde{\nu} \approx 700 \text{ cm}^{-1}$. This is more clearly evident in π polarization (Figure 4), where the vibronic intensity mechanism has apparently broadened out finer details. We can account for the σ_1 structure (Figure 3) by involving a subprogression in $\Delta\tilde{\nu} \approx 400 \text{ cm}^{-1}$. This assignment is not at all unique, though we do emphasize that these weak undulations in the band profile are highly reproducible.

Fortunately, an independent determination of the Franck-Condon-active vibrational modes is available from the resonance Raman work of Strekas and Spiro.⁸ These workers found that system II excitation of $[(\text{NH}_3)_5\text{Co}]_2^{5+}$ in aqueous solution gave resonance enhancement of vibrational modes at 1108 and 500 cm^{-1} assigned respectively to the symmetric $\nu(\text{O}_2)$ and $\nu(\text{Co-O})$ stretches. We therefore assign our ~ 700 - and ~ 400 - cm^{-1} progressions to the analogous excited-state $\nu(\text{O}_2)$ and $\nu(\text{Co-O})$ modes.

The dramatic reduction in excited-state $\nu(\text{O}_2)$ is consistent with the formally one-electron-reduced character of the O_2 unit in the MLCT excited state. Using ground- and excited-state $\nu(\text{O}_2)$ frequencies as indicated above, we calculated⁹ the intensities of the $\nu(\text{O}_2)$ vibronic progression, approximating the O_2 unit as a diatomic harmonic oscillator. Experimental relative intensities for the 0-0, 0-1, and 0-2 transitions of 1/1.8/1.3 (which roughly describes both σ_1 and π polarizations) are reproduced by a calculation in which $|\Delta Q| = 0.15 \text{ \AA}$. With the ground-state O-O distance being 1.29 \AA , the excited-state O-O distance is therefore estimated to be about 1.44 \AA . For comparison, the planar (μ -peroxo)dinuclear cobalt(III) ion $[(\text{NH}_3)_5\text{Co}]_2^{4+}$ has an O-O distance of 1.469 \AA in its thiocyanate salt¹⁰ and an O-O stretching frequency of $\sim 800 \text{ cm}^{-1}$.¹¹ Both the estimated distortion and the stretching frequency of the excited state thus indicate an O-O bond order close to that of a peroxo-bridged dinuclear cobalt(III) center.

We note that another assignment once suggested¹² for system II, $\pi \rightarrow \pi^*$ "localized" in the bridging superoxide, is much less consistent with our observations. The $\pi \rightarrow \pi^*$ transition of O_2^- in alkali halide lattices¹³ reaches its

(5) Day, P.; Orchard, A. F.; Thompson, A. J.; Williams, R. J. P. *J. Chem. Phys.* **1965**, *42*, 1973.

(6) In labeling the d orbitals we choose the local Co axes with z parallel to Co-O and x parallel to the cation C_2 axis.

(7) (a) Hunziker, H. E.; Wendt, H. R. *J. Chem. Phys.* **1974**, *60*, 4622. (b) Becker, K. H.; Fink, E. J.; Langen, P.; Schurath, U. *Ibid.* **1974**, *60*, 4623.

(8) Strekas, T. C.; Spiro, T. G. *Inorg. Chem.* **1975**, *14*, 1421.

(9) (a) Henderson, J. R.; Muramoto, M.; Willett, R. A. *J. Chem. Phys.* **1964**, *41*, 580. (b) Yersin, H.; Otto, H.; Zink, J. I.; Gliemann, G. *J. Am. Chem. Soc.* **1980**, *102*, 951.

(10) Fronczek, F. R.; Schaefer, W. P.; Marsh, R. E. *Acta Crystallogr., Sect. B* **1974**, *B30*, 117.

(11) Barraclough, C. G.; Lawrance, G. A.; Lay, P. A. *Inorg. Chem.* **1978**, *17*, 3317.

(12) Garbett, K.; Gillard, R. D. *J. Chem. Soc. A* **1968**, 1725.

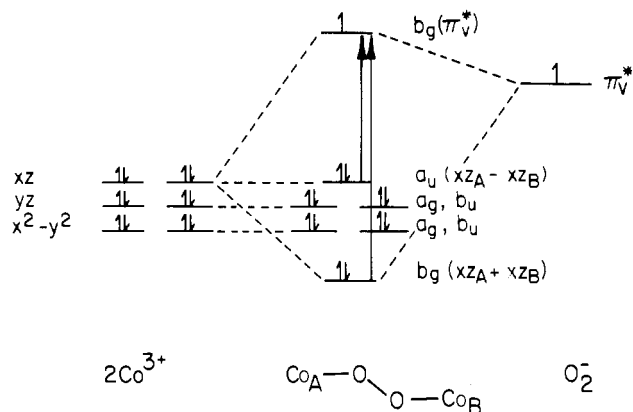


Figure 5. Molecular orbital diagram of the interaction of Co(III) $d\pi$ orbitals with $\pi_v^*(\text{O}_2^-)$ for a C_{2h} [CoO_2Co] unit. The MLCT transitions discussed in the text are indicated by arrows.

Franck-Condon maximum at about 10 quanta of a progression in a $\nu(\text{O}-\text{O})$ frequency of 575 cm^{-1} , and the excited-state distortion is 0.43 \AA , conforming to the formal excited-state bond order of only 0.5.

The π polarization (Figure 4) shows a second, weaker progression in a 700-cm^{-1} interval beginning at $17\,200\text{ cm}^{-1}$. These features are also evident in σ polarization (Figure 3) at about the same frequencies. The splitting from the main progression of $\sim 3000\text{ cm}^{-1}$ could conceivably be attributed to a $\nu(\text{N}-\text{H})$ mode. However, the Raman studies⁸ did not reveal such a resonance-enhanced frequency nor is strong Franck-Condon activity for such a mode very palatable.

We suggest that this feature can be understood in terms of another MLCT transition, as described by the MO diagram of Figure 5. The only strong interactions of π_v^* with Co(III) $d\pi$ orbitals should be with xz , and as a result, two $xz \rightarrow \pi^*$ MLCT transitions should be reasonable. The allowed (and lowest energy) transition is associated with the nonbonding xz combination, which is a familiar feature of "three-center" bonding as in, for example, $\text{M}-\text{O}-\text{M}$ complexes.¹⁴ We assign the weak transition beginning at $17\,200\text{ cm}^{-1}$ (Figure 4) to the bonding to antibonding MLCT transition, $b_g \rightarrow b_g$. The intensity of this forbidden transition in both π and σ polarizations should be vibronically induced. Just as for system I, the drastic temperature behavior of the stronger absorption bands has prevented us from checking this prediction.

The 3000-cm^{-1} splitting of the two MLCT absorptions is thus indicated to be a measure of the strength of the π -back-bonding interaction of O_2^- with the Co(III) centers. Clearly, this is a substantial fraction of the total π^* splitting of $\sim 12\,500\text{ cm}^{-1}$ (determined by the energy of system I). We note that π^* splittings (presumably σ only) of ~ 7000 ⁷ and $\sim 8000\text{ cm}^{-1}$ ¹⁵ have been reported for HO_2^- and H_2O_2 , respectively, which are results that are consistent with our interpretation.¹⁶ Furthermore, the relatively high intensity of the allowed MLCT transition also demonstrates the impor-

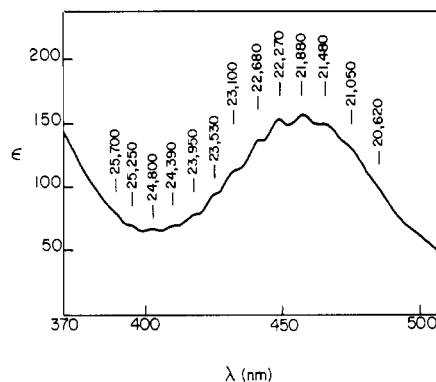


Figure 6. Absorption spectrum of a $6.1\text{ }\mu\text{m}$ thick crystal of [$(\text{N}-\text{H}_3)_5\text{Co}$] $_2\text{O}_2$](NO_3) $_2\text{Cl}_3 \cdot 2\text{H}_2\text{O}$ in π polarization at 11 K .

tance of π back-bonding to the superoxide ligand.

System III

System III appears strongly in both π and σ polarizations but with differing intensities and λ_{max} values (Figures 2 and 3). The integrated intensity clearly decreases at low temperature in both polarizations, indicating the intensity to be at least partially vibronically induced.

At low temperature the π spectrum shows a long progression with an average interval of $420 \pm 10\text{ cm}^{-1}$ (Figure 6); unfortunately, the 0-0 region is obscured by other absorption systems. There is some weak structure in the σ_1 spectrum (and also in the σ_2 spectrum¹⁷), but these features are exactly coincident with structure in the π spectrum.

Room-temperature σ_1 and σ_2 absorption maxima are coincident at $\sim 480\text{ nm}$, and, taking rough account of the effects of intense absorption to longer and shorter wavelengths, the intensities are approximately equal. This suggests (Table III) that the 480-nm transition is σ polarized parallel to $\text{Co}-\text{O}$. The predominant π polarization of the structured absorption (room-temperature absorption maximum in π polarization at 464 nm) suggests " \perp $\text{Co}-\text{O}$ " polarization, the last entry in Table III.

All of these results are beautifully consistent with the previous assignment¹ of system III to the " $^1A_{1g} \rightarrow ^1T_{1g}$ " Co(III)-localized ligand field transition. In local tetragonal symmetry, this transition splits into $^1A_1 \rightarrow ^1E$ ($xz, yz \rightarrow z^2$) and $^1A_1 \rightarrow ^1A_2$ ($x^2 - y^2 \rightarrow xy$) components. With a predominant vibronic intensity-giving mechanism,¹⁸ the $^1A_1 \rightarrow ^1E$ transition generally proves¹⁹ to be predominantly local- z -axis polarized, whereas $^1A_1 \rightarrow ^1A_2$ turns out to be nearly exclusively x and y polarized. Thus, we attribute the structured π absorption to " $^1A_1 \rightarrow ^1A_2$ ", with the stronger σ absorption due to " $^1A_1 \rightarrow ^1E$ ", contaminated with some " $^1A_1 \rightarrow ^1A_2$ " structured absorption.

The " $^1A_1 \rightarrow ^1A_2$ " transition, $x^2 - y^2 \rightarrow xy$, is purely equatorial, so only Franck-Condon activity of equatorial $\text{Co}-\text{N}$ modes is expected. As the equatorial $\text{Co}-\text{N}$ bonds are structurally equivalent to those of [$\text{Co}(\text{NH}_3)_6$] $^{3+}$, it is most satisfying that both the absorption maximum and detailed vibronic structure are very similar to those of the $^1A_{1g} \rightarrow ^1T_{1g}$ transition of [$\text{Co}(\text{NH}_3)_6$] $^{3+}$ in the salt studied by Wilson and Solomon.²⁰ The absence of structure in the " $^1A_1 \rightarrow ^1E$ " transition is reasonable because it would be blurred both by simultaneous activation of $\text{Co}-\text{N}$ and $\text{Co}-\text{O}$ modes in this axial transition and by any splitting²¹ of the degenerate " 1E " state.

(13) Ibezawa, M.; Rolfe, J. *J. Chem. Phys.* **1973**, *58*, 2024.
 (14) Baumann, J. A.; Meyer, T. *J. Inorg. Chem.* **1980**, *19*, 345.
 (15) Osafune, K.; Kimura, K. *Chem. Phys. Lett.* **1974**, *25*, 47.
 (16) Our model suggests that the MLCT transition of a mononuclear Co(III)- O_2^- complex should be blue-shifted relative to the corresponding bridged dicobalt(III) complex, as only a single $xz \rightarrow \pi_v^*$ MLCT (allowed bonding-antibonding) transition then exists. This is consistent with the reported spectra (Gillard, R. D.; De Jesus, J. D. P.; Tipping, L. R. *H. J. Chem. Soc., Chem. Commun.* **1977**, *58*) of the Rh(III) superoxo complexes [$(\text{CIRh}(\text{en})_2)_2\text{O}_2$] $^{3+}$ ($\lambda_{\text{max}} = 545\text{ nm}$) and [$(\text{CIRh}(\text{en})_2)_2\text{O}_2$] $^{2+}$ ($\lambda_{\text{max}} = 485\text{ nm}$). For [$\text{Co}(\text{CN})_5\text{O}_2$] $^{3-}$ (McLendon, G.; Pickens, S. R.; Martell, A. E. *Inorg. Chem.* **1977**, *16*, 1551), a very weak band is reported near the energy of the intense MLCT transition¹ of [$(\text{Co}(\text{CN})_5\text{O}_2$] $^{2-}$, but this is, in our opinion, plausibly attributable to a trace of the dinuclear species. Alternatively, it might be due to a forbidden transition such as $yz \rightarrow \pi_v^*$ (Figure 5).

(17) As noted in the Experimental Section, our low-temperature σ_2 spectra were affected by light-leak artifacts. However, vibronic structure similar to that in σ_1 polarization was evident in the data.
 (18) Ballhausen, C. J.; Moffitt, W. *J. Inorg. Nucl. Chem.* **1956**, *3*, 178.
 (19) Yamada, S. *Coord. Chem. Rev.* **1967**, *2*, 83.
 (20) Wilson, R. B.; Solomon, E. I. *J. Am. Chem. Soc.* **1980**, *102*, 4085.

Finally, we note that Yamada gives¹⁹ $^1A_1 \rightarrow ^1A_2$ and $^1A_1 \rightarrow ^1E$ maxima for the $[\text{Co}(\text{NH}_3)_5(\text{NCS})]^{2+}$ ion of 465 and 483 nm. Thus, our earlier conclusion¹ that the ligand field strength of bridging O_2^- is near that of N-bound NCS^- appears to have been correct (but see footnote 21).

System IV

For a low-temperature glassy solution,¹ system IV appears as a shoulder ($\epsilon \approx 3500$, $\lambda_{\text{max}} \approx 345$ nm) on a very intense ($\epsilon = 23\,960$) absorption band maximizing at 301 nm. Nujol mulls and KBr pellets of the title compound show features of similar energies and relative intensities at low temperature.

Figure 3 shows that a shoulder ($\epsilon \approx 400$) is resolved at 350 nm in the low-temperature π spectrum. We were unable to extend our σ spectra into this region but can infer from the weakness of the π feature that there must be a strong σ -polarized feature in order to account for the high isotropic ϵ at 345 nm.

This polarization behavior supports a " $^1A_{1g} \rightarrow ^1T_{2g}$ " ligand field assignment;¹ the weak π -polarized transition is assigned to the " $^1A_1 \rightarrow ^1B_2$ " ($x^2 - y^2 \rightarrow z^2$) component, whereas the presumed intense σ transition would be " $^1A_1 \rightarrow ^1E$ " ($xz, yz \rightarrow xy$), with polarizations following¹⁹ in exact analogy to those of system III. The absence of any vibronic structure prevents more conclusive assignments but is consistent with the similarly unstructured $^1A_{1g} \rightarrow ^1T_{2g}$ transition of $[\text{Co}(\text{NH}_3)_6]^{3+}$ ($\lambda_{\text{max}} = 345$ nm) in the low-temperature study by Wilson and Solomon.²⁰

An alternative assignment was suggested in a review,²² namely, the LMCT transition $\pi_v^*(\text{O}_2) \rightarrow d\sigma^*$. However, the available data do not support this assignment²³ because the most intense transition of this type is expected²⁴ to be $\pi_v^* \rightarrow z^2$ ($b_g \rightarrow b_u$), which would be π polarized. It is likely that all

the $\pi_v^*(\text{O}_2) \rightarrow d\sigma^*$ transitions fall at higher energies ($\lambda < 300$ nm) because of unfavorable electron-repulsion effects.²²

Finally, we note that we could scan to 300 nm in π polarization (Figure 3) without any sign of an intense absorption maximum. The very intense absorption maximum seen at ~ 300 nm in isotropic spectra must therefore be σ polarized, as expected from the LMCT [$\pi_h^* \rightarrow z^2$ ($a_g \rightarrow b_u$)] assignment given previously.¹

Conclusions

The results of the present study confirm the essential features of our original interpretation¹ of the electronic spectra of (μ -superoxo)dicobalt(III) complexes. In addition, our work has established that the O_2 unit is a potent π acceptor (as well as a π donor²⁵), which is in agreement with simple electronic structural models.^{1,22} It is remarkable that with the variety of bonding interactions available to the superoxide, the spectroscopic oxidation state of cobalt, as judged by ligand field transitions, remains unmistakably Co(III). The fact that this conclusion accords with structural results and with EPR data is very satisfying.

Another finding of much interest is that the MLCT state is unquestionably peroxide-like. The localization of the excited electron in the ligand is analogous to that inferred²⁶ for the MLCT excited state of $\text{Ru}(\text{bpy})_3^{2+}$. Unfortunately, we cannot tell from the data in hand whether the "hole" in the dicobalt MLCT state is localized on a single Co or not. The $\nu(\text{O}_2)$ of the excited state is somewhat lower than that of a normal peroxide, suggesting that the O–O bond is activated in some way. However, no notable photochemistry has yet been observed²⁷ for this MLCT excitation.

Acknowledgment. This research was supported by National Science Foundation Grants CHE81-20419 and CHE82-18502 (H.B.G., V.M.M.) and by National Institutes of Health Grant HL-12395 (W.P.S.). B.D.S. acknowledges support from the California Institute of Technology as a Myron A. Bantrell Research Fellow in Chemistry, 1981–1983.

Registry No. $[(\text{NH}_3)_5\text{Co}(\text{O}_2)](\text{NO}_3)_2\text{Cl}_3 \cdot 2\text{H}_2\text{O}$, 87870-95-9.

Supplementary Material Available: Tables of anisotropic thermal parameters and structure factor amplitudes (14 pages). Ordering information is given on any current masthead page.

(21) Figure 5 suggests that a component (one-fourth?) of " $^1A_1 \rightarrow ^1E$ " should be shifted 3000 cm^{-1} to higher energy, or to ~ 400 nm. This interpretation is overly naive as the MLCT state splittings are not simple one-electron parameters. The experimental data neither exclude nor support such large ligand field splittings.

(22) Lever, A. B. P.; Gray, H. B. *Acc. Chem. Res.* **1978**, *11*, 348.

(23) It was suggested in ref 22 that a ligand field assignment for system IV should be excluded because an analogue of the title complex with histidine ligands showed a corresponding feature in its CD spectrum, whereas the octahedral $^1A_{1g} \rightarrow ^1T_{2g}$ is magnetic dipole forbidden. However, this argument is not compelling because mononuclear Co(III)-amino acid complexes may have quite respectable CD intensity associated with $^1A_{1g} \rightarrow ^1T_{2g}$ (Denning, R. G.; Piper, T. S. *Inorg. Chem.* **1966**, *5*, 1056), presumably because of a symmetry much lower than O_h .

(24) Miskowski, V. M.; Gray, H. B. *Inorg. Chem.* **1975**, *14*, 401.

(25) Tovrog, B. S.; Drago, R. S. *J. Am. Chem. Soc.* **1974**, *96*, 6765.

(26) Bradley, P. G.; Kress, N.; Hornberger, B. A.; Dallinger, R. F.; WOODRUFF, W. H. *J. Am. Chem. Soc.* **1981**, *103*, 7441.

(27) Valentine, J. S.; Valentine, D. *J. Am. Chem. Soc.* **1971**, *93*, 1111.